

Slippery but tough - the rapid fracture of lubricated frictional interfaces

E. Bayart,¹ I. Svetlizky,¹ and J. Fineberg¹

¹The Racah Institute of Physics, The Hebrew University of Jerusalem, Jerusalem, Israel

(Dated: December 3, 2024)

We study the onset of friction for rough contacting blocks whose interface is coated with a thin lubrication layer. High speed measurements of the real contact area and stress fields near the interface reveal that propagating shear cracks mediate lubricated frictional motion. While lubricants reduce interface strengths, surprisingly, they significantly increase energy dissipated, Γ , during rupture. Moreover, lubricant viscosity affects the onset of friction but has *no* effect on Γ . Fracture mechanics provide a new way to view the otherwise hidden complex dynamics of the lubrication layer.

PACS numbers: 46.55.+d, 46.50.+a, 62.20.Qp, 81.40.Pq

Lubrication of solid surfaces is generally used to reduce frictional resistance to sliding motion and to prevent material wear [1]. Effects of fluids on the frictional properties of an interface are of particular significance in geophysics, since tectonic faults are generally lubricated by interstitial water or melted rocks [2–4]. Along spatially extended interfaces, which are considered here, much fundamental understanding of the collective mechanisms responsible for the reduction of friction due to lubrication is still lacking [5–7]. While the sliding dynamics of lubricated systems is an active field of research [8–10], the mechanisms mediating their transition from stick to slip remain largely unexplored. At the microscopic level, stick-slip mechanisms have been discussed for decades [11, 12]. Within single contacts, very thin films, typically less than 10 molecular layers, exhibit strongly enhanced apparent viscosity caused by surface-induced alignment of the fluid molecules [13–15]. Along spatially extended rough interfaces, the real contact area is defined by a large ensemble of single contacts (asperities) that couple contacting elastic blocks. The real contact area, A , is generally orders of magnitude smaller than the apparent one [1, 16, 17]. In the plastic deformation regime within dry interfaces, A is proportional to applied normal loads, as the local pressure at each contact is constrained to the plastic limit of the bulk material [1, 17]. Here we consider rough surfaces in the boundary lubrication regime, where the contacting surfaces are covered by a thin lubricant layer [18]. The discrete asperities in this regime still bear the entire normal load; they are not entirely immersed in the fluid layer as in the full lubrication regime. The mixed lubrication regime is an intermediate region, where the normal load is partially borne by solid contacts and partially by the liquid layer.

In dry friction, the onset of motion is mediated by rupture fronts propagating along the frictional interface [19, 20]. These fronts are true (singular) shear cracks; the strain fields during their propagation are well-described by Linear Elastic Fracture Mechanics (LEFM) [21]. Frictional rupture arrest is also governed by the same framework [22, 23]. Here, we examine the mechanisms coming into play when motion initiates within *lubricated* inter-

faces, in the boundary lubrication regime. We first find that interface rupture still corresponds to the singular shear cracks described by LEFM. While reducing static friction by facilitating rupture nucleation, we will show that, surprisingly, lubricants make solid contacts effectively tougher, increasing the fracture energy of the interface (the dissipated energy per unit crack extension). Moreover, while the macroscopic frictional resistance of the interface depends on the lubricant viscosity, the fracture energy does not.

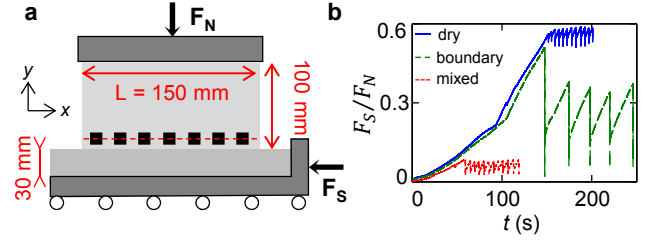


FIG. 1: Experimental setup and stick-slip behavior. (a) Normal F_N and shear F_S forces are applied to contacting PMMA blocks. Shear is applied uniformly via translation of a rigid stage. Strain gage rosettes measure the 3 components of the 2D-strain tensor at 14 locations along and 3.5 mm above the interface, while the real contact area is measured optically. (b) Loading curves, F_S/F_N vs time, are plotted for typical experiments, with $F_N = 4000$ N: dry (solid blue line), boundary lubricated (dashed green line) and, for comparison, in the mixed lubricated regime (dotted red line). The lubricant used is a hydrocarbon oil (TKO-77).

We describe experiments where two blocks of poly(methylmethacrylate) (PMMA) are first pressed together with normal forces, F_N , of $2500 < F_N < 7000$ N. Shear forces, F_S , are then applied uniformly, as the bottom block is translated via a rigid stage, until stick-slip motion initiates (Fig. 1). A detailed description of the setup is given in [21]. PMMA has a rate-dependent Young’s modulus $3 < E < 5.6$ GPa and Poisson ratio $\nu_p = 0.33$. PMMA’s Rayleigh wave speed is $c_R = 1255$ ms^{-1} for plane strain conditions. Top and bottom blocks have respective $x \times y \times z$ dimensions $150 \times 100 \times 5.5$ mm and $200 \times 30 \times 30$ mm. The contact-

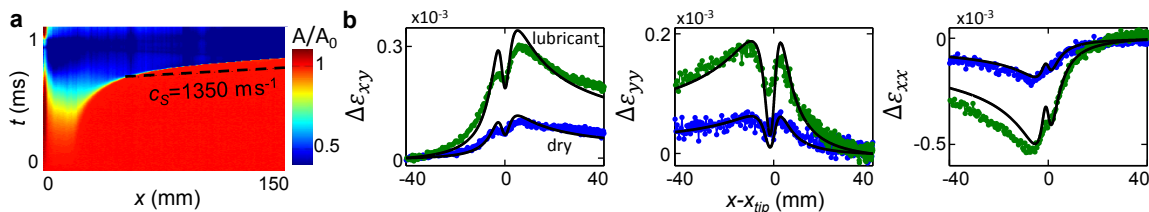


FIG. 2: Singular interfacial shear cracks govern friction initiation. (a) The spatio-temporal evolution of the contact area $A(x, t)$ of a typical lubricated interface (hydrocarbon oil, TKO-77). Each line is a snapshot in time of $A(x, t)$, normalized by $A_0 = A(x, 0)$ immediately prior to the event. Here, a rupture accelerates to a propagation velocity $c_f = 0.92 c_R$. The rupture tip, $x_{tip}(t)$ are the locations where $A(x, t)$ drops sharply. (b) Variation of the strain field $\Delta\varepsilon_{ij}(x - x_{tip})$ with the distance from rupture tips, x_{tip} , for ruptures propagating along dry (blue line) and lubricated (green line, rupture presented in (a)) interfaces. In both, the applied normal stress was $\langle\sigma_{yy}\rangle = 7 \pm 0.5$ MPa and strains were measured at $x = 77$ mm, where $c_f \sim 0.3 c_R$. Black solid lines are fits to the LEFM solution for $y = 3.5$ mm (Eq. 1). The only fitting parameter is the fracture energy; $\Gamma_{dry} = 2.6 \pm 0.3 \text{ J m}^{-2}$ for the dry and $\Gamma_{lub} = 23 \pm 3 \text{ J m}^{-2}$ for the lubricated interfaces.

ing flat surfaces of the top and bottom blocks were (top) optically smooth and (bottom) with a surface roughness of $0.5 \mu\text{m}$ r.m.s. During each sliding event, an array of 14 strain gages recorded the 3 components of the 2D-strain tensor, ε_{ij} , 3.5 mm above the interface, each at 10^6 samples/s. Corresponding stresses, σ_{ij} , are calculated from ε_{ij} after accounting for the viscoelasticity of PMMA (see [23]). In parallel, the real area of contact, $A(x, t)$, was measured at 1000×8 locations at 580000 frames/s, using an optical method based on total internal reflection (see [21]) where incident light only traverses the interface at contacts, and is otherwise reflected.

Experiments of lubricated friction were performed using silicone oils with kinematic viscosities, $\nu = 5, 100$ and $10^4 \text{ mm}^2 \text{ s}^{-1}$ and a hydrocarbon oil (TKO-77, Kurt J. Lesker Company) of $\nu \sim 200 \text{ mm}^2 \text{ s}^{-1}$. Lubricants were applied to either or both of the contacting surfaces and then wiped. Our results are not appreciably affected by the wiping procedure (number of wipes, application or not between experiments). PMMA and the lubricants used are nearly index-matched: PMMA-1.49, TKO-77-1.48, and silicone oils-1.42. Hence, under total internal reflection, incident light will be totally transmitted where gaps between asperities are filled with liquid. At the onset of motion, the observed contact area variations (see below), demonstrate that air, not lubricant, fills the gaps between contacts. This provides validation that the experiments take place in the boundary lubrication regime.

When sheared, the lubricated system undergoes stick-slip motion (Fig. 1b). Drops of F_S in the loading curves correspond to slip events with macroscopic relative displacement of the blocks. The lubricant layer affects the macroscopic frictional resistance, reducing the static friction coefficient (i.e. the shear force threshold). The amplitudes of the force drops, however, are larger than for dry friction. In the boundary lubrication regime, this pattern is extremely robust, and is independent of the nature and quantity of the lubricant. For completeness, a typical loading curve in the mixed lubrication regime is

included in Fig. 1b, where F_S/F_N thresholds are further reduced. Motion in this regime is not addressed here.

As in dry friction, each sliding event in the boundary lubrication regime is preceded by propagating rupture fronts that break the solid contacts forming the interface, as shown in Fig. 2a. Macroscopic sliding only occurs when a front traverses the entire interface [23–26]. For steady rupture fronts moving at a velocity c_f , $\varepsilon_{ij}(x, t) = \varepsilon_{ij}(x - c_f t)$. Using this and the optically identified location of the rupture tip, $x_{tip}(t)$, we converted $\varepsilon_{ij}(x, t)$ to spatial measurements $\varepsilon_{ij}(x - x_{tip})$ [21]. As in the example of Fig. 2b (blue line), rupture fronts in dry friction are shear cracks whose stress field variations, $\Delta\sigma_{ij}(r, \theta)$, are quantitatively described by LEFM, with respect to the crack tip ($r = 0$) [21]:

$$\Delta\sigma_{ij}(r, \theta) = \frac{K_{II}(c_f)}{\sqrt{2\pi r}} \Sigma_{ij}^{II}(\theta, c_f), \quad (1)$$

where $\Sigma_{ij}^{II}(\theta, c_f)$ is a universal angular function and the coefficient, $K_{II}(c_f)$, is called the stress intensity factor [27]. $\Delta\sigma_{ij}$ expresses the stress changes between the initially applied and residual stresses along the frictional crack faces. $\Delta\sigma_{ij}$ are related to measured strain variations $\Delta\varepsilon_{ij}$ via the dynamic Young's modulus and Poisson ratio of PMMA. LEFM relates K_{II} to the fracture energy, Γ , the energy dissipated per unit crack advance; $K_{II} \propto f(c_f)\sqrt{\Gamma}$, where $f(c_f)$ is a known universal function [27].

In Fig. 2b we compare measurements of $\Delta\varepsilon_{ij}(x - x_{tip})$ during rupture front propagation for dry and lubricated interfaces. As Fig. 2b explicitly shows, the agreement between measured $\Delta\varepsilon_{ij}(x - x_{tip})$ for the *lubricated* interface and the LEFM solution is excellent. Hence, ruptures propagating along a lubricated interface are shear cracks. Surprisingly, Γ , for the same applied normal load, is an order of magnitude *greater* for the lubricated interface, Γ_{lub} , than for the dry one, Γ_{dry} . For the examples presented in Fig. 2b, $\Gamma_{lub} = 23 \pm 3 \text{ J m}^{-2}$ while $\Gamma_{dry} = 2.6 \pm 0.3 \text{ J m}^{-2}$. In Fig. 3a we present

$\Delta\varepsilon_{ij}(x-x_{tip})$ for dry and lubricated (hydrocarbon) interfaces, when rescaled by $1/\sqrt{\Gamma}$. We find that the rescaled dry and lubricated strain fields are *identical*.

What determines Γ ? In dry friction Γ grows linearly with the normal load [1, 23]. Extracting Γ from the rescaling procedure, Fig. 3b shows that Γ indeed remains proportional to the average normal stress, $\langle\sigma_{yy}\rangle$, in the boundary lubrication regime. Moreover, the value of Γ is *unaffected* by the lubricant viscosity; Γ is *constant* for viscosity variations of $5 < \nu < 10^4 \text{ mm}^2 \text{ s}^{-1}$ in silicon oils. We do, however, find that Γ strongly depends on the lubricant composition; TKO-77 has values of Γ about 3 times larger than all of the silicon oils used. For a given c_f , increased values of Γ induce increased shear stress drops during rupture propagation. We note that the increased shear force drops in loading curves (e.g. Fig. 1b) are partially caused by this large stress drop, with the remainder due to motion after the rupture passage.

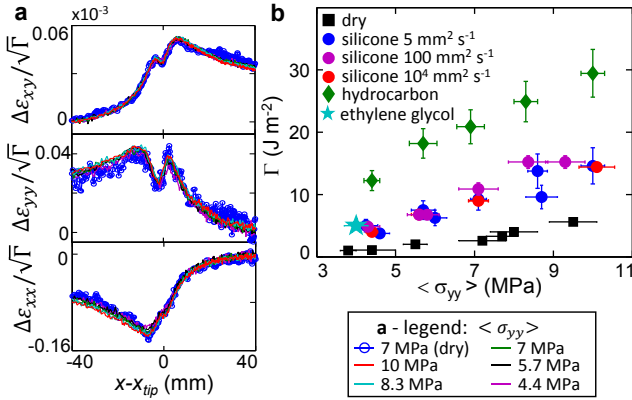


FIG. 3: Dependence of the fracture energy with normal stress. (a) Comparison of $\Delta\varepsilon_{ij}(x-x_{tip})$ for dry and lubricated experiments, when normalized by $\sqrt{\Gamma}$, for different normal loads. Units are $(\text{Pa m})^{-1/2}$. Superimposed are the dry experiment in Fig. 2b and 5 lubricated (TKO-77) experiments where $c_f \sim 0.3c_R$ with $\langle\sigma_{yy}\rangle$ as in the legend, yielding $\Gamma_{dry} = 2.6 \text{ J m}^{-2}$ and $\Gamma_{TKO} = 12.3, 18.2, 23, 25$ and 29.5 J m^{-2} . (b) Γ is measured by fitting the strain field with the LEFM solution (as in (a)) for both dry and lubricated interfaces vs F_N . All Γ vary linearly with F_N , Γ is independent of the lubricant viscosity while highly dependent on lubricant composition.

Why does the lubricant *increase* Γ ? We consider the simplest (linear slip-weakening) description of the dissipative zone near a rupture tip [28]. Rupture occurs when the shear stress on the interface reaches the maximal (regularized) value σ_{xy}^{peak} . Slip is then initiated and σ_{xy} is reduced to the residual value σ_{xy}^{res} over a slip distance d_c , typically the asperity size. In this model, the fracture energy is expressed as $\Gamma = \frac{1}{2}(\sigma_{xy}^{peak} - \sigma_{xy}^{res})d_c$. More sliding occurs after the rupture passed, dissipating more energy. Therefore, the energy dissipated by the rupture is only part of the total energy dissipated during a slip event. An increase of Γ can be induced by increased

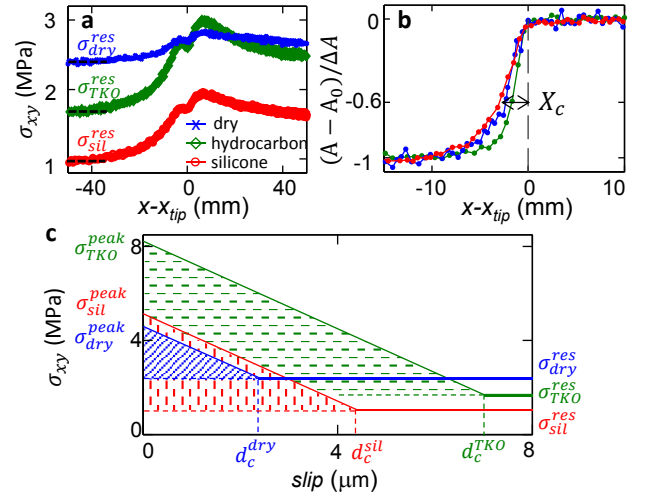


FIG. 4: Increase of Γ and the slip-weakening model. (a) Shear stress as a function of the distance from x_{tip} for ruptures propagating ($c_f \sim 0.3c_R$) along a dry (blue crosses) and lubricated interfaces with hydrocarbon oil (green diamonds) and silicone oil with $\nu = 10^4 \text{ mm}^2 \text{ s}^{-1}$ (red circles). $\Gamma = 2.6, 9$ and 23 J m^{-2} for respectively dry, silicone and hydrocarbon oils for $\langle\sigma_{yy}\rangle = 7 \text{ MPa}$. (b) Reduction of the contact area $A - A_0$, normalized by the total drop in A , $\Delta A = A_0 - A_{res}$, as a function of the distance from x_{tip} for the three experiments in (a). The dissipative zone size X_c is defined as the length scale where a 60% drop of ΔA occurs. (c) Diagram of the linear slip-weakening model [28]. Respectively for dry and lubricated with silicone and hydrocarbon oils interfaces, residual stresses, defined in (a), are 2.4, 1 and 1.7 MPa, peak stresses σ_{xy}^{peak} , using Eq. 2, are 4.6, 5.1 and 8.2 MPa and d_c are 2.4, 4.4 and $7 \mu\text{m}$. Integration over the blue (green, red) hatched areas provides the dry (lubricated) fracture energy.

values of either σ_{xy}^{peak} or d_c , or a decrease of σ_{xy}^{res} . σ_{xy}^{res} is indeed strongly reduced by the lubricant (Fig. 4a). The magnitude of the reduction relative to the dry interface depends on the nature of the lubricant, greater for silicone oil than for TKO-77. While we can not measure σ_{xy}^{peak} directly, as our strain gages are located above the interface [21], we can estimate it knowing the size of the dissipative zone. Indeed, following the linear slip-weakening model [28]:

$$\sigma_{xy}^{peak} = \sigma_{xy}^{res} + \sqrt{\frac{9\pi}{32} \frac{\Gamma E}{(1-\nu_p^2) X_c}} \quad (2)$$

where X_c is the dissipative zone size, the distance behind the crack tip over which contacts are being broken. X_c is the scale over which $A(x)$ drops from its initial to residual value. In Fig. 4b we compare X_c for dry and lubricated experiments (see [21] for details). We find that X_c is not significantly affected by the lubricant layer; its value (for $c_f \sim 0.3c_R$) is approximately 3 mm. Inserting this value in Eq. 2, we see that σ_{xy}^{peak} is *not* reduced by the lubricant and is even significantly increased when TKO-77 is used (Fig. 4c). The linear slip-weakening model also

indicates that d_c increases when interfaces are lubricated. This simple model therefore explains the increase in Γ by increased stress drops, $\sigma_{xy}^{peak} - \sigma_{xy}^{res}$, coupled to larger slip distances d_c that are due to the presence of a lubricant.

The fact that σ_{xy}^{peak} is not reduced by the lubricant provides evidence that the lubricant does not behave as a fluid, as fluids can not sustain shear. Highly compressed fluids are known to experience large increases of viscosity with pressure, either due to jammed long chains [29, 30], or to pressure-induced layering transitions [13–15]. As a consequence, the fluid layer may mechanically acquire shear strength as the local pressure between contacting asperities approaches PMMA’s yield stress (~ 500 MPa). Our results suggest that, by these means, the trapped lubricant is able to sustain shear stress during the loading of the system. Consequently, the rupture mechanisms of the interlocked solid asperities are similar to the dry interface; asperities are plastically deformed prior to sliding of the surfaces [21]. Once rupture propagation initiates slip, the trapped lubricant will lose its induced shear strength, because of either rearrangement of the lubricant molecules [11, 31] or slip-induced heating of the contacts [3, 32]. In this phase, slip is *facilitated* by the lubricant, consequently increasing the release of the elastic energy stored in the material, resulting in reduced σ_{xy}^{res} (Fig. 4).

Such a transition from stick to slip in terms of a crystallization and melting transition of the lubricant has been discussed for single micro-contacts [11, 33], as well as for a multi-contact interface [34], although there has been some question whether a melting transition indeed occurs when a contact slides [12, 31]. Our results suggest that this scenario may, in fact, take place. Alternatively, one might think about effects of pore pressure, induced by fluids filling the contacts. Pore pressure would reduce σ_{xy}^{res} [2] by reducing the effective normal stress at the contact level, hence it would increase Γ . Calculations, however, suggest that pore pressure may require longer time scales than those available during rupture [35] to become established.

We have shown that in the boundary lubrication regime, the macroscopic frictional resistance is reduced (Fig. 1b) but the contacts actually become tougher, requiring a larger amount of energy (Γ) to break (Fig. 3). These intriguing results are not contradictory; rupture nucleation and dissipation are independent processes. Rupture nucleation determines the initial stress levels and therefore, the interface’s “static” frictional strength. Although nucleation is the key to understanding initial interfacial strength, processes determining its origin remain enigmatic [36, 37].

Fig. 5 demonstrates that the lubricant viscosity solely determines the initial stress σ_{xy}^{pre} needed to nucleate the rupture. Using silicone oils of different viscosities, where all experiments were performed with the same normal stress profile, Fig. 5 reveals that the higher ν , the lower σ_{xy}^{pre} , while σ_{xy}^{res} does *not* depend on ν . σ_{xy}^{pre} deter-

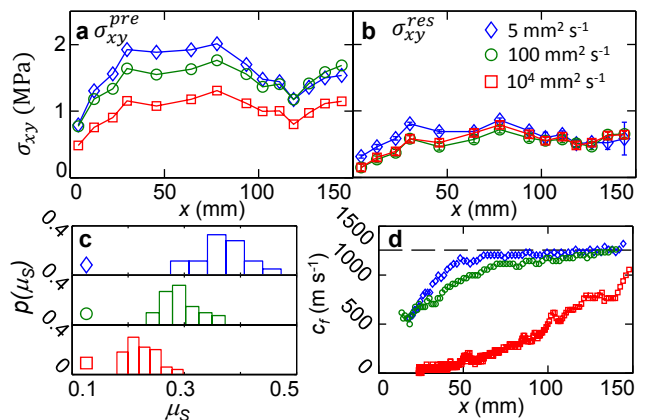


FIG. 5: Dependence of the macroscopic frictional resistance with ν . Profiles of (a) the initial σ_{xy}^{pre} and (b) residual stresses σ_{xy}^{res} for interfaces lubricated with silicone oils having $\nu = 5$ (diamonds), 100 (circles) and 10^4 (squares) $\text{mm}^2 \text{s}^{-1}$. Normal stress distributions are identical for the three experiments and $\Gamma = 6.7 \pm 0.3 \text{ J m}^{-2}$. σ_{xy}^{res} does not depend on the viscosity of the silicone oil. (c) Histograms of the static friction coefficient μ_s of sliding events for lubricated interfaces with silicone oils of different viscosity. Around 50 events are considered for each ν . Higher ν yield lower frictional resistance. (d) 3 examples of $c_f(x)$ for the lubricants in (a) and (b). The larger ν , the slower the front. Dashed line denotes c_R . Symbols and colors in (a-d) as in (b).

mines the static friction coefficient $\mu_s = F_S/F_N$. Hence (Fig. 5c) μ_s is significantly dependent on ν , as suggested by earlier studies [1, 38].

As Γ and σ_{xy}^{res} are ν -independent (Figs. 3 and 5b), LFM predicts that the only effect of σ_{xy}^{pre} should be on the rupture dynamics. A larger σ_{xy}^{pre} yields faster rupture fronts [27] as verified in both dry friction [39] and in ice-quakes [40]. This is born out by the examples shown in Fig. 5d; for the same σ_{yy} profile, the higher ν , the lower σ_{xy}^{pre} , and the slower the rupture front. Our results imply that the reduction of μ_s is purely the result of rupture front nucleation at a reduced threshold, due to higher ν . Lower initial stresses do not prevent interfacial rupture as long as the elastic energy stored by block deformation is sufficiently above the energy dissipated during the rupture process (Fig. 4c).

We have shown that, in the boundary lubrication regime, while macroscopic frictional resistance is reduced, an interface actually becomes considerably tougher, as Γ increases by up to an order of magnitude relative to dry interfaces. Our simple model provides a qualitative explanation for these intriguing observations, but it is simply a conjecture; and there may well be alternative explanations. Obtaining a fundamental understanding of both the dynamics of frictional interfaces and their associated dissipative properties presents a needed and interesting challenge.

We acknowledge support from the James S. McDonnell

Fund Grant 220020221, the European Research Council (Grant No. 267256) and the Israel Science Foundation (Grants 76/11 and 1523/15). E.B. acknowledges support from the Lady Davis Trust. We thank G. Cohen for comments.

-
- [1] F. P. Bowden and D. Tabor, *The Friction and Lubrication of Solids* (Oxford Univ. Press, New York, 2001), 2nd ed.
- [2] J. R. Rice, *J. Geophys. Res. - Solid Earth* **111**, B05311 (????).
- [3] H. Noda, E. M. Dunham, and J. R. Rice, *J. Geophys. Res. - Solid Earth* **114**, B07302 (2009).
- [4] R. C. Viesca and D. I. Garagash, *Nature Geosc.* **8**, 875 (2015).
- [5] D. A. Rigney and S. Karthikeyan, *Tribol. Lett.* **39**, 3 (2010).
- [6] L. Pastewka, S. Moser, P. Gumbsch, and M. Moseler, *Nature Mater.* **10**, 34 (2011).
- [7] N. N. Gosvami, J. A. Bares, F. Mangolini, A. R. Konicek, D. G. Yablon, and R. W. Carpick, *Science* **348**, 102 (2015).
- [8] B. N. J. Persson, *Sliding Friction Physical Principles and Applications* (Springer-Verlag, New York, 2000), 2nd ed.
- [9] S. Campen, J. Green, G. Lamb, D. Atkinson, and H. Spikes, *Tribol. Lett.* **48**, 237 (2012).
- [10] A. Ernesto, D. Mazuyer, and J. Cayer-Barrioz, *Tribol. Lett.* **59**, 23 (2015).
- [11] P. A. Thompson and M. O. Robbins, *Science* **250**, 792 (1990).
- [12] I. Rosenhek-Goldian, N. Kampf, A. Yeredor, and J. Klein, *Proc. Natl Acad. Sci. USA* **112**, 7117 (2015).
- [13] S. Granick, *Science* **253**, 1374 (1991).
- [14] J. Klein and E. Kumacheva, *Science* **269**, 816 (1995).
- [15] B. Bhushan, J. N. Israelachvili, and U. Landman, *Nature* **374**, 607 (1995).
- [16] J. Greenwood and J. Williams, *Proc. R. Soc. Lond. A* **295**, 300 (1966).
- [17] J. H. Dieterich and B. D. Kilgore, *Tectonophysics* **256**, 219 (1996).
- [18] B. Hamrock, S. Schmid, and B. Jacobson, *Fundamentals of fluid film lubrication* (CRC Press, 2004).
- [19] S. M. Rubinstein, G. Cohen, and J. Fineberg, *Nature* **430**, 1005 (2004).
- [20] K. Xia, A. J. Rosakis, and H. Kanamori, *Science* **303**, 1859 (2004).
- [21] I. Svetlizky and J. Fineberg, *Nature* **509**, 205 (2014).
- [22] D. S. Kammer, M. Radiguet, J. P. Ampuero, and J. F. Molinari, *Tribol. Lett.* **57**, 23 (2015).
- [23] E. Bayart, I. Svetlizky, and J. Fineberg, *Nature Phys.* (2015), advance online publication.
- [24] S. M. Rubinstein, G. Cohen, and J. Fineberg, *Phys. Rev. Lett.* **98**, 226103 (2007).
- [25] O. M. Braun, I. Barel, and M. Urbakh, *Phys. Rev. Lett.* **103**, 194301 (2009).
- [26] J. Tromborg, J. Scheibert, D. S. Amundsen, K. Thogersen, and A. Malthe-Sorensen, *Phys. Rev. Lett.* **107**, 074301 (2011).
- [27] L. B. Freund, *Dynamic Fracture Mechanics* (Cambridge, New York, 1990).
- [28] C. Palmer, A. and R. Rice, *J.*, *Proc. R. Soc. Lond. A* **332**, 527 (1973).
- [29] H. Everett, *S.A.E. Journal* **41** (1937).
- [30] G. W. Stachowiak and A. W. Batchelor (Butterworth-Heinemann, Burlington, 2006).
- [31] A. Dhinojwala, S. C. Bae, and S. Granick, *Tribol. Lett.* **9**, 55 (2000).
- [32] O. Ben-David, S. M. Rubinstein, and J. Fineberg, *Nature* **463**, 76 (2010).
- [33] Y. Lei and Y. Leng, *Phys. Rev. Lett.* **107**, 147801 (2011).
- [34] T. Baumberger and C. Caroli, *Eur. Phys. J. B* **4**, 13 (1998).
- [35] N. Brantut and J. R. Rice, *Geophys. Res. Lett.* **38**, L24314 (2011).
- [36] Z. P. Yang, H. P. Zhang, and M. Marder, *Proc. Natl Acad. Sci. USA* **105**, 13264 (2008).
- [37] S. Latour, A. Schubnel, S. Nielsen, R. Madariaga, and S. Vinciguerra, *Geophys. Res. Lett.* **40**, 5064 (2013).
- [38] W. Hardy, *Collected Works* (Cambridge University Press, 1936).
- [39] O. Ben-David, G. Cohen, and J. Fineberg, *Science* **330**, 211 (2010).
- [40] J. I. Walter, I. Svetlizky, J. Fineberg, E. E. Brodsky, S. Tulaczyk, C. G. Barcheck, and S. P. Carter, *Earth and Planetary Science Letters* **411**, 112 (2015).